# Influence of self-steepening and intrapulse Raman scattering on modulation instability in oppositely directed coupler

A. K. Shafeeque Ali, K. Porsezian,* and T. Uthayakumar
*Department of Physics, Pondicherry University, Pondicherry 605014, India*
(Received 27 May 2014; published 13 October 2014)

We investigate the modulation instability in oppositely directed coupler in the presence of higher-order effects. Using linear stability analysis, we obtain an expression for instability gain. Special attention is paid to find out the influence of self-steepening effect and intrapulse Raman scattering on modulation instability. The study shows that in normal dispersion, regime instability gain exists even if perturbation frequency ($\Omega$) is zero. But the instability gain at $\Omega = 0$ is zero, when the dispersion is anomalous. Moreover, self-steepening effect and intrapulse Raman scattering form new instability regions and, hence, provide a new way to generate solitons or ultrashort pulses. Further, efficient control of modulation instability by adjusting self-steepening effect and intrapulse Raman scattering also successfully demonstrated.

DOI: 10.1103/PhysRevE.90.042910 PACS number(s): 05.45.−a, 42.65.Dr, 42.65.Sf, 42.65.Wi

## I. INTRODUCTION

Nonlinear directional couplers (NDCs) have attracted widespread interest due to their potential applications in signal processing, including optical switching and logic operation [1,2]. In 1982, Jensen first suggested the model of nonlinear coupler, which consists of two wave guides in close proximity, which can allow the possibility of desired redistribution of waves between the channels [1]. Tunnel penetration of electro magnetic wave from one channel to another channel of coupler causes coupling between the wave guides after a particular distance known as coupling length and direction of light propagation is preserved [3,4]. In the case of conventional couplers, propagation of the input and output fields are in the same direction [1,5]. If any one of the channel of NDCs is replaced with negative index material then the coupler is known as oppositely directed coupler because the direction of input and output optical modes become opposite [6]. So it can act like a mirror [7]. Oppositely directed couplers exhibit the phenomenon of optical bistability and admit gap solitons due to an effective feedback mechanism in negative index channel arising from the oppositely directed phase velocity and energy flow [6]. Based on the model of coupled modes, the nonlinear propagation of electromagnetic wave in oppositely directed coupler has been theoretically investigated [8].

The phenomenon of modulation instability (MI) was first discovered by T. Brooke Benjamin and Jim E. Feir for periodic surface gravity waves [9]. Now it has been widely observed in most of the nonlinear systems like nonlinear optics [10–14], plasma [15–17], and Bose Einstein condensates [18–20]. MI arises due to an interplay between nonlinearity and group velocity dispersion in temporal domain and due to interaction between nonlinearity and diffraction in spatial domain [21]. During this process small perturbation imposed on a continuous wave grows exponentially and this leads to beam breakup in either space or time. MI in conventional NDCs has been investigated for both normal and anomalous group velocity dispersion regimes and it is reported that even at vanishing modulation frequency instability gain exists [5]. MI in oppositely directed coupler were also discussed and results are quite different from that observed in conventional couplers made up of same materials [22,23]. It has been found that MI in oppositely directed coupler is highly affected by the ratio of forward and backward propagating wave's power and nonlinear parameters [22]. Unlike normal dispersion regime, MI generation is thresholdless for ratio of forward and backward propagating wave's power in anomalous group velocity dispersion regime, and increase in the input power suppresses the MI gain [22]. Saturable nonlinearity can be used to control the generation of side bands through the oppositely directed coupler [23].

In the context of directional coupler, the MI analysis is deeply connected with the nonlinear Schrödinger equation (NLSE), which leads to the formation of soliton or solitary wave. When we consider the higher-order effects in oppositely directed coupler, an extended wave equation is required. Our main aim is to discuss the MI in oppositely directed coupler with higher-order effects. In this paper, we will discuss the impact of higher-order nonlinear effects like self-steepening and intrapulse Raman scattering on modulation instability in oppositely directed coupler. We will extend our study in both normal and anomalous group velocity dispersion regimes. The rest of the paper is organized as follows. In Sec. II, the theoretical model of the problem and linear stability analysis leading to dispersion relation are presented. Investigation of effect of self-steepening on MI and investigation of effect of intrapulse Raman scattering on MI in oppositely directed coupler are carried out in detail in Sec. III and Sec. IV, respectively. Conclusions are made in Sec. V.

## II. THEORETICAL MODEL

The coupled envelope equation of nonlinear Schrödinger type is one of the major theoretical models that has been considered so far to describe the physics of electromagnetic wave propagation inside the coupler. When the peak power of propagating electromagnetic wave inside the coupler is above the threshold level, the higher-order effects play an important role. So the propagation model should be modified accordingly. We consider the effect of self-steepening and

*ponzsol@yahoo.com

 

intrapulse Raman scattering in the propagation model and study its effect on modulation instability. Self-steepening arises from intensity dependence of group velocity and it creates an optical shock on the trailing edge of the pulse in the absence of group velocity dispersion. During the process of intrapulse Raman scattering, low-frequency components of the pulse are amplified by Raman gain due to transfer of energy from high-frequency component of same pulse and pulse spectrum shifts toward the low-frequency side [5]. It is well known that the third-order dispersion contributes none to the MI gain [24]. So, for this particular work of investigation of modulation instability, third-order linear dispersion is trivial. If we neglect the cross-phase modulation effect, the model that describes the propagation of electromagnetic wave in oppositely directed coupler is given by following coupled nonlinear Schrödinger equation (CNSE) [5,6]:

$$i\,\sigma_1\frac{\partial u_1}{\partial z}-\frac{\beta_{21}}{2}\frac{\partial^2 u_1}{\partial t^2}+k_{12}\,u_2\,e^{-i\delta z}+\gamma_1\Bigg[(|u_1|^2)\,u_1 +i\,s_1\frac{\partial(|u_1|^2u_1)}{\partial t}-T_{R1}\,u_1\frac{\partial(|u_1|^2)}{\partial t}\Bigg]=0, \tag{1}$$

$$i\,\sigma_2\frac{\partial u_2}{\partial z}-\frac{\beta_{22}}{2}\frac{\partial^2 u_2}{\partial t^2}+k_{21}\,u_1\,e^{i\delta z}+\gamma_2\Bigg[(|u_2|^2)u_2 +i\,s_2\frac{\partial(|u_2|^2u_2)}{\partial t}-T_{R2}\,u_2\frac{\partial(|u_2|^2)}{\partial t}\Bigg]=0. \tag{2}$$

Where $\sigma_1$ and $\sigma_2$ indicate the sign of refractive index in channel-1 and channel-2 of the coupler, respectively. We consider channel-1 is made by positive index material (PIM) and channel-2 by negative index material (NIM), hence $\sigma_1=1$ and $\sigma_2=-1$; $u_1(z,t)$ and $u_2(z,t)$ are the normalized complex amplitude of the modes in PIM and NIM channels, respectively; $\gamma_1$ and $\gamma_2$ are the nonlinear coefficient, respectively; $k_{12}$ and $k_{21}$ are coupling coefficients; $\beta_{21}$ and $\beta_{22}$ are group velocity dispersion coefficients. And $\delta=\beta_1-\beta_2$, where $\beta_1$ and $\beta_2$ represent the propagation constants of the individual channels. In the case of oppositely directed coupler with NIM channel, the wave guides are not identical and hence $\beta_1\neq\beta_2$. If the channels of the coupler are identical then $\delta=0$. The last two terms are responsible for self-steepening and the Raman-induced frequency shift, induced by intrapulse Raman scattering, respectively.

### A. Linear stability analysis

We use linear stability analysis to study MI in oppositely directed coupler based on Eqs. (1) and (2) as in Refs. [22,23,25,26]. The basic idea of linear stability analysis is to perturb continuous wave solution and then analyze whether this small perturbation grows or decays with propagation. Assuming the following form of steady-state solutions to Eqs. (1) and (2):

$$a_1=u_1\exp(i\,q\,z)\exp\Big(-i\,\frac{\delta}{2}z\Big), \tag{3}$$

$$a_2=u_2\exp(i\,q\,z)\exp\Big(i\,\frac{\delta}{2}z\Big). \tag{4}$$

The linear stability of steady state can be examined by perturbing the solutions of the following form:

$$a_1=[u_1+\alpha_1(z,t)]\exp(i\,q\,z)\exp\Big(-i\,\frac{\delta}{2}z\Big), \tag{5}$$

$$a_2=[u_2+\alpha_2(z,t)]\exp(i\,q\,z)\exp\Big(i\,\frac{\delta}{2}z\Big). \tag{6}$$

Where the complex field $\alpha_j(z,t)\ll u_j$, $j=1,2$. Substituting Eqs. (5) and (6) into Eqs. (1) and (2) and linearizing, we obtain

$$i\,\frac{\partial\alpha_1}{\partial z}-i\,\frac{\beta_{21}}{2}\frac{\partial^2\alpha_1}{\partial t^2}+k_{12}\,\alpha_2-k_{12}\,f\alpha_1+\frac{p}{1+f^2}\,\gamma_1 \times\Bigg[(\alpha_1+\alpha_1^*)+2\,i\,s_1\frac{\partial\alpha_1}{\partial t}-T_{R1}\frac{\partial\alpha_1}{\partial t}\Bigg]=0, \tag{7}$$

$$-i\,\frac{\partial\alpha_2}{\partial z}-i\,\frac{\beta_{22}}{2}\frac{\partial^2\alpha_2}{\partial t^2}+k_{21}\,\alpha_1-k_{21}\,f^{-1}\,\alpha_2+\frac{p}{1+f^2}\,f^2\,\gamma_2 \times\Bigg[(\alpha_2+\alpha_2^*)+2\,i\,s_2\frac{\partial\alpha_2}{\partial t}-T_{R2}\frac{\partial\alpha_2}{\partial t}\Bigg]=0, \tag{8}$$

where $f=\frac{u_2}{u_1}$, which describes how the total power $p=u_1^2+u_2^2$ is divided between forward and backward propagating waves. In order to solve the above set of two linear differential equations, we assume a plane-wave ansatz, consisting of two sideband components with forward and backward propagation having the form

$$\alpha_j(z,t)=c_j\,\{\exp[i\,(K\,z-\Omega\,t)]\} +d_j\,\{\exp[-i\,(K\,z-\Omega\,t)]\}, \tag{9}$$

where $K$ and $\Omega$ are wave-vector and frequency of perturbation amplitude. Substituting Eq. (9) into Eqs. (7) and (8), we obtain a set of four linearly coupled equations satisfied by $c_j$ and $d_j$. This set has nontrivial solution only when $4\times4$ determinant formed by coefficient matrix vanishes as given below:

$$\begin{pmatrix} m_{11} & m_{12} & m_{13} & m_{14}\\ m_{21} & m_{22} & m_{23} & m_{24}\\ m_{31} & m_{32} & m_{33} & m_{34}\\ m_{41} & m_{42} & m_{43} & m_{44}\end{pmatrix}\begin{pmatrix} c_1\\ c_2\\ d_1\\ d_2\end{pmatrix}=0,$$

where $m_{11}=0$, $m_{12}=R\,f^2\,\gamma_2$, $m_{13}=k_{21}$, $m_{14}=R\,f^2\,\gamma_2(1-2\,s_2\,\Omega-i\,T_{R2}\,\Omega)-K-k_{21}\,f^{-1}+\frac{\beta_{22}}{2}\,\Omega^2$, $m_{21}=R\,\gamma_1$, $m_{22}=0$, $m_{23}=R\,\gamma_1\,(1-2\,s_1\,\Omega-i\,T_{R1}\,\Omega)+K-k_{12}\,f-\frac{\beta_{21}}{2}\,\Omega^2$, $m_{24}=k_{12}$, $m_{31}=k_{21}$, $m_{32}=R\,f^2\,\gamma_2\,(1+2s_2\,\Omega+i\,T_{R2}\,\Omega)+K-k_{21}\,f^{-1}-\frac{\beta_{22}}{2}\,\Omega^2$, $m_{33}=0$, $m_{34}=R\,f^2\,\gamma_2$, $m_{41}=R\,\gamma_2\,(1+2\,s_1\,\Omega+i\,T_{R1}\,\Omega)-K-k_{12}\,f-\frac{\beta_{21}}{2}\,\Omega^2$, $m_{42}=k_{12}$, $m_{43}=R\,\gamma_1$, $m_{44}=0$, and $R=\frac{p}{1+f^2}$. Vanishing condition of above $4\times4$ stability matrix leads to a fourth-order polynomial in $K$ as given below,

$$K^4+a\,K^3+b\,K^2+c\,K+d=0. \tag{10}$$

The four roots of Eq. (10) determine the stability of the continuous-wave solution. In order to observe MI, one of the roots of the above fourth-order polynomial should possesses a nonzero and negative imaginary part that corresponds to an exponential growth of amplitude of the perturbation. The

instability gain is given by the equation [25]

$$g = |\mathrm{Im}(K)|, \tag{11}$$

where $\mathrm{Im}(K)$ denotes the imaginary part of $K$.

## III. EFFECT OF SELF-STEEPENING ON MODULATION INSTABILITY

Here, we will discuss the influence of self-steepening effect on MI in oppositely directed coupler. In this section, initially we omit the Raman self-scattering effect by setting $T_{R1} = T_{R2} = 0$. We consider both negative and positive index channels of the coupler are nonlinear with $\gamma_1 = \gamma_2 = 1/$ (kW m). In order to study the effect of self-steepening, we consider the following cases. Case 1: Both channels are not influenced by self-steepening effect ($s_1 = 0$ and $s_2 = 0$). Case 2: One of the channels is influenced by self-steepening effect and the other is not ($s_1 = 0$ and $s_2 \neq 0$ or $s_1 \neq 0$ and $s_2 = 0$). Case 3: Both channels are influenced by self-steepening effect and are equal ($s_1 = s_2 \neq 0$). Case 4: Both channels are influenced by self-steepening effect but opposite in sign ($s_1 = -s_2 \neq 0$). We discuss the above-mentioned cases for both normal and anomalous group velocity dispersion regimes.

### A. Normal group velocity dispersion regime

As an illustrative example, we select $k_{12} = 10\ \mathrm{m}^{-1}$, $k_{21} = 10\ \mathrm{m}^{-1}$, and $p = 10$ kW. Here, we consider MI in normal group velocity dispersion regime, so we select $f = 1$ and $\beta_{21} = \beta_{22} = 1\ \mathrm{ps}^2\,\mathrm{m}^{-1}$. Figure 1(a) depicts the instability gain versus perturbation frequency without self-steepening effect ($s_1 = s_2 = 0$). From the figure it is clear that instability spectra consists of single conventional MI band centered at zero perturbation frequency formed by balance between group velocity dispersion and self-phase modulation. If any one of the channel of the coupler is influenced by self-steepening effect, the maximum gain and band width of conventional MI band reduces [27]. Also, it is very interesting to observe new instability regions are formed as shown in Fig. 1(b). These instability regions are MI bands induced by self-steepening effect. Figure 1(c) corresponds to when both channels are influenced by equal self-steepening effect. In this case also new instability regions are observed, but it is shifted to high perturbation frequency. Finally if both channels are influenced by equal self-steepening but opposite sign, then instability gain spectra resemble case 1, as shown in Fig. 1(d). Here, the effect of self-steepening of two channels cancel each other, and no new instability regions are observed.

It can be concluded from Fig. 1 that, in normal dispersion regime, instability gain exists even if perturbation frequency is zero and instability gain at $\Omega = 0$ is constant in all four cases. Self-steepening effect form new instability regions and hence provide a new way to generate solitons or ultrashort pulses. It is already reported that, in the case of two core optical fiber self-steepening effect can shift MI band [24]. Our result also shows similar shifting of instability band. So, MI can be effectively controlled by adjusting self-steepening effect.

### B. Anomalous group velocity dispersion regime

When the dispersion is anomalous, then the parameters are $f < 0$, $\beta_{21} < 0$, and $\beta_{22} < 0$. So as an illustrative example,

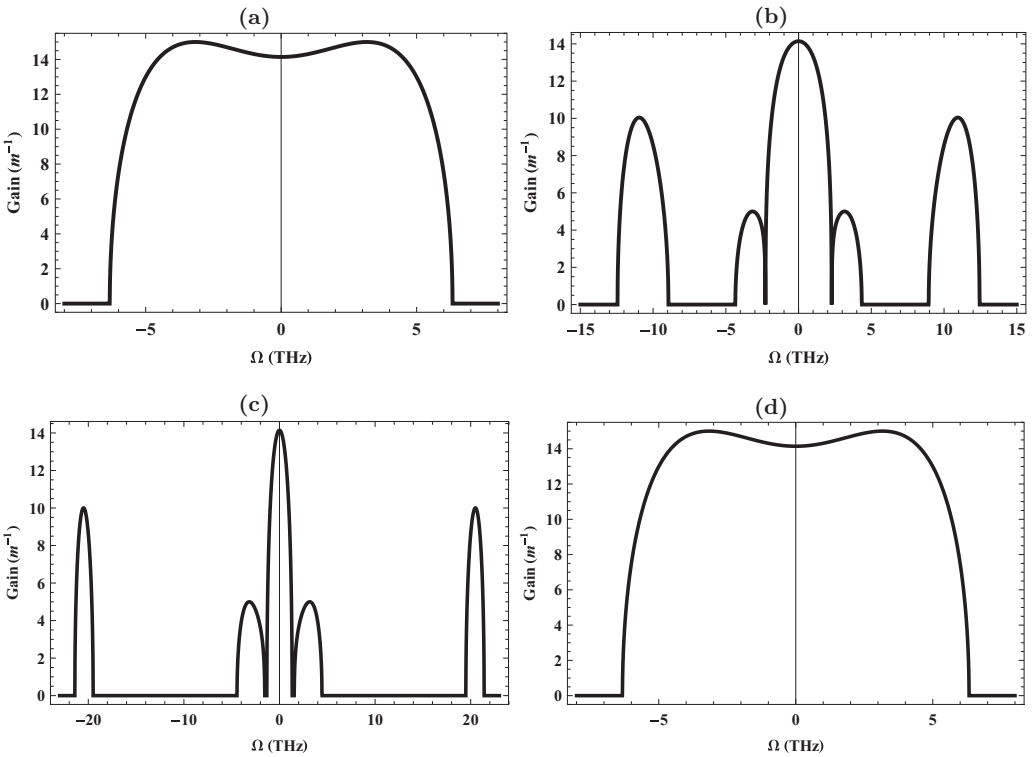


FIG. 1. Instability gain spectra in normal group velocity dispersion regime under different combinations of $s_1$ and $s_2$ when $p = 10$ kW, and $k_{12} = k_{21} = 10\ \mathrm{m}^{-1}$. (a) $s_1 = 0$ ps/(kW m), $s_2 = 0$ ps/(kW m), (b) $s_1 = 0$ ps/(kW m), $s_2 = 1$ ps/(kW m), (c) $s_1 = 1$ ps/(kW m), $s_2 = 1$ ps/(kW m) and (d) $s_1 = 1$ ps/(kW m), $s_2 = -1$ ps/(kW m).

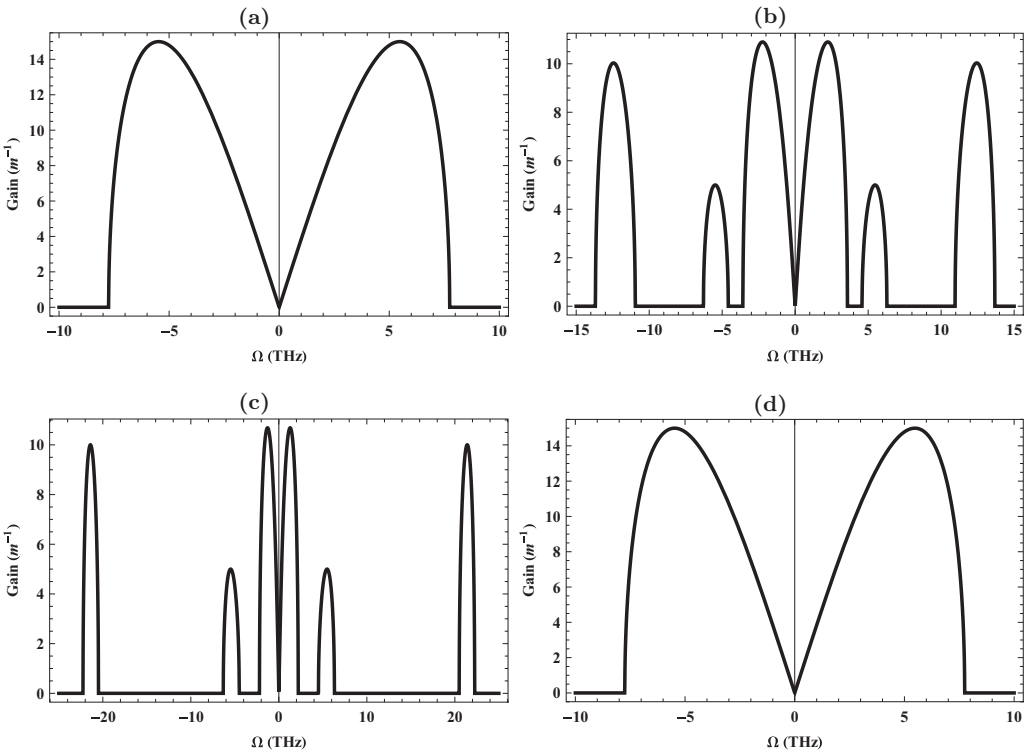


FIG. 2. Instability gain spectra in anomalous group velocity dispersion regime under different combinations of $s_1$ and $s_2$ when $p = 10$ kW, and $k_{12} = k_{21} = 10$ m$^{-1}$. (a) $s_1 = 0$ ps/(kW m), $s_2 = 0$ ps/(kW m), (b) $s_1 = 0$ ps/(kW m), $s_2 = 1$ ps/(kW m), (c) $s_1 = 1$ ps/(kW m), $s_2 = 1$ ps/(kW m) and (c) $s_1 = 1$ ps/(kW m), $s_2 = -1$ ps/(kW m).

we select $f = -1$, $\beta_{21} = -1$ ps$^2$ m$^{-1}$, and $\beta_{22} = -1$ ps$^2$ m$^{-1}$. The main difference here from normal dispersion is that there is no instability gain at zero perturbation frequency, as shown in Fig. 2. The instability spectra are centered around zero perturbation frequency. When any one of the channel is influenced by self-steepening effect, then the maximum gain and band width of conventional MI band reduces and new instability regions are formed on either side of zero perturbation frequency as shown in Fig. 2(b). If both channels are influenced by self-steepening effect, then new instability regions are formed in higher perturbation frequency than in case 2, as in the case of normal dispersion regime as depicted in Fig. 2(c). When both channels are influenced by equal and opposite self-steepening effect then the MI gain is same as self-steepeningless case.

The influence of self-steepening on MI is basically same in both anomalous and normal dispersion regime. Self-steepening effect form new instability regions and hence, it provides a new way to generate solitons or ultrashort pulses. But, the instability gain at $\Omega = 0$ is zero and is observed when the dispersion is anomalous.

## IV. EFFECT OF INTRAPULSE RAMAN SCATTERING ON MODULATION INSTABILITY

Here, we study in detail the effect of intrapulse Raman scattering on MI in oppositely directed couplers. For this particular study, we neglect the role of self-steepening effect. Figures 3(a) and 3(b) depict the MI in normal and anomalous

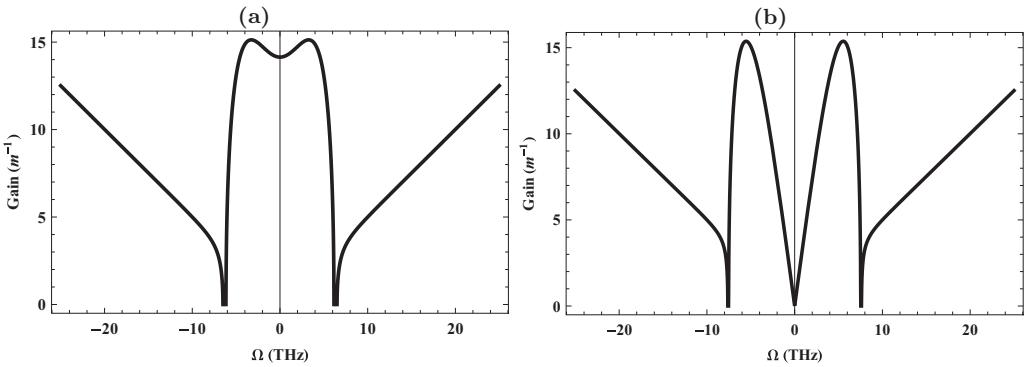


FIG. 3. Instability gain spectra showing the effect of intrapulse Raman scattering in (a) normal group velocity dispersion regime and (b) anomalous group velocity dispersion regime when $p = 10$ kW, and $k_{12} = k_{21} = 10$ m$^{-1}$, $s_1 = s_2 = 0$ ps/(kW m), and $T_{R1} = T_{R2} = 0.1$ ps/(kW m).

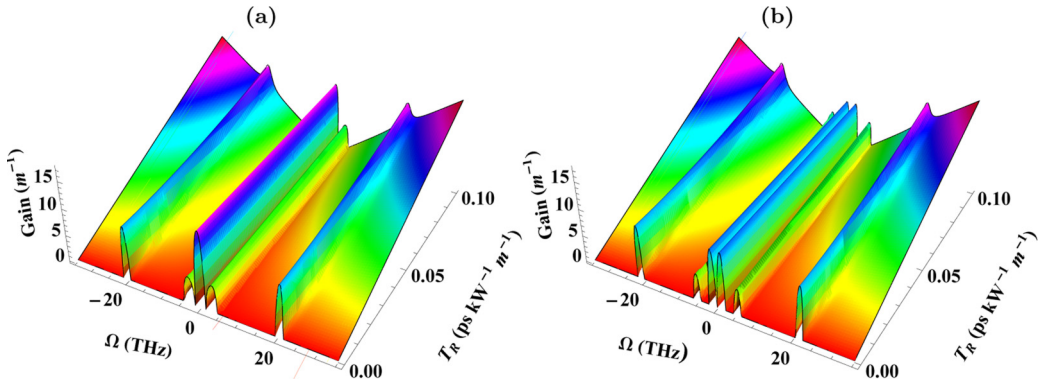


FIG. 4. (Color online) Instability gain spectra showing the combined effect of self-steepening and intrapulse Raman scattering in (a) normal group velocity dispersion regime and (b) anomalous group velocity dispersion regime, when $p = 10$ kW, $k_{12} = k_{21} = 10$ m$^{-1}$, and $s_1 = s_2 = 1$ ps/(kW m).

group velocity dispersion regimes, respectively, where the parameters are $T_{R1} = T_{R2} = 0.1$ ps/(kW m). It is already reported that intrapulse Raman scattering forms additional MI regions with small growth rates but wide spans for higher frequencies in microstructured fiber [28], and additional MI band with linearly increasing gain with perturbation frequency in the dispersion decreasing fibers [29]. Nonconventional MI side bands are more prone to Raman-induced degradations than ordinary MI side bands [30]. From Fig. 3 it is clear that due to intrapulse Raman scattering, additional MI regions for higher frequencies appear. So new instability regions are induced by intrapulse Raman scattering and it widens the extent of MI. Instability gain of these regions increases linearly as perturbation frequency increases. Also, the effect of intrapulse Raman scattering is the same for both normal and anomalous group velocity dispersion regimes.

Figure 4 depicts instability gain spectra versus perturbation frequency and intrapulse Raman scattering in normal and anomalous dispersion regime, when $p = 10$ kW, $k_{12} = k_{21} = 10$ m$^{-1}$ and $s_1 = s_2 = 1$ ps/(kW m). These figures show the combined effect of self-steepening and intrapulse Raman scattering on MI gain. As explained in previous sections, at lower perturbation frequency, instability gain spectra consists of conventional MI band formed by the balance between group velocity dispersion and self-phase modulation. One can notice the effect of self-steepening on MI gain spectra as the form of new instability region at higher perturbation frequency. It is also clear from figures that when the magnitude of intrapulse Raman scattering increases, additional MI bands are formed with linearly increasing gain. So self-steepening and intrapulse Raman scattering form additional instability regimes at higher perturbation frequencies and widen the extent of MI.

## V. CONCLUSION

Based on the coupled mode equations and linear stability analysis, we have investigated the modulation instability in oppositely directed coupler with higher-order effects. We have extended our study in both normal and anomalous group velocity dispersion regimes. It is found that in a normal dispersion regime, instability gain exists even if perturbation frequency is zero. On the other hand, for the case of an anomalous dispersion regime, the instability gain is zero at vanishing perturbation frequency. From the study on influence of self-steepening effect and intrapulse Raman scattering, we have found that those effects form new instability regions and widen the extent of modulation instability. So these effects provide a new way to generate solitons or ultrashort pulses. Also, the effect of self-steepening and intrapulse Raman scattering is the same for both normal and anomalous group velocity dispersion regimes.

## ACKNOWLEDGMENTS

K.P. thanks CSIR, DST, IFCPAR, and NBHM, Government of India agencies, for financial support through research projects. A. K. Shafeeque Ali thanks DST FIST, Government of India, for the financial support through PURSE scheme.

## APPENDIX

The coefficients of Eq. (10) are given by where

$$a = 2\,\Omega\,R\,[2\,(\gamma_2\,f^2\,s_2 - \gamma_1\,s_1) + 2\,i\,(\gamma_2\,T_{R2}\,f^2 - \gamma_1\,T_{R1})], \tag{A1}$$

$$b = 2\,R\,f\,(\gamma_1\,k_{12} + \gamma_2\,k_{21}) - \left(k_{12}\,f - \frac{k_{21}}{f}\right)^2 + \Omega^2\left[k21\left(\beta_{21}\,f + \frac{\beta_{22}}{f}\right) - R\,(\gamma_1\,\beta_{21} + \gamma_2\,f^2\,\beta_{22})\right.$$
$$+ 4\,R^2\,(\gamma_1^2\,s_1^2 - 4\,\gamma_1\,\gamma_2\,s_1\,s_2\,f^2 + \gamma_2^2\,s_2^2\,f^4 - \gamma_1^2\,T_{R1}^2 + f^2\,\gamma_1\,\gamma_2\,T_{R1}\,T_{R2} - f^2\,\gamma_2^2\,T_{R2}^2 - i\,T_{R1}\,\gamma_1\,(2f^2\,\gamma_2\,s_2 - \gamma_1\,s_1)$$
$$\left. - i\,T_{R2}\,\gamma_2\,f^2\,(2\,s_1\,\gamma_1 - s_2\,\gamma_2\,f^2))\right] - \frac{\Omega^4}{4}\,[\beta_{21}^2 + \beta_{12}^2], \tag{A2}$$

$$
\begin{aligned}
c = \Omega\Big[ & 2R\left(2k_{21}^2\frac{s_1}{f^2} - 2k_{21}k_{12}\gamma_1 s_1 - 2k_{12}^2\gamma_2 s_2 + 2k_{21}k_{12}f^2\gamma_2 s_2 - ik_{21}k_{12}\gamma_1 T_{R1} + ik_{21}^2\frac{\gamma_1 T_{R1}}{f^2} - if^4k_{12}^2\gamma_2 T_{R2}\right.\\
& \left. + ik_{21}k_{12}f^2\gamma_2 T_{R2}\right) + 4R^2(2f^3\gamma_1\gamma_2 k_{12}s_2 - 2f\gamma_2\gamma_1 k_{21}s_1 - if\gamma_2\gamma_1 k_{21}T_{R1} + if^3\gamma_1\gamma_2 k_{21}T_{R2})\Big]\\
& + 4\Omega^3\Big[R\left(\beta_{21}f^3k_{12}\gamma_2 s_2 - \frac{\gamma_1 s_1}{f}\beta_{22}k_{21} - \frac{i}{2f}\beta_{22}k_{21}\gamma_1 T_{R1} + \frac{i}{2}\beta_{21}f^3k_{12}\gamma_2 T_{R2}\right) + R^2\left(\beta_{22}\gamma_1\gamma_2 s_1 f^2\right.\\
& \left. - \beta_{21}\gamma_1\gamma_2 s_2 f^2 + \frac{i}{2}\beta_{22}\gamma_1\gamma_2 f^2 T_{R1} - \frac{i}{2}\beta_{21}\gamma_1\gamma_2 f^2 T_{R2}\right) + R^3\left(4f^2\gamma_1^2\gamma_2 s_1^2 s_2 - 4f^4\gamma_1\gamma_2^2 s_2^2 s_1 + 4i\gamma_1^2\gamma_2 s_1 s_2 T_{R1}f^2\right.\\
& - 2i\gamma_1\gamma_2^2 s_2^2 T_{R1}f^4 - \gamma_1\gamma_2 s_2 T_{R1}^2 f^2 + 2i\gamma_1^2\gamma_2 s_1^2 T_{R2}f^2 - 4i\gamma_1\gamma_2^2 s_1 s_2 T_{R2}f^4 - \gamma_1^2\gamma_2 2s_1 T_{R1}T_{R2}f^2\\
& \left.\left. + 2\gamma_1\gamma_2^2 s_2 T_{R1}T_{R2}f^4 - \frac{i}{2}\gamma_1^2\gamma_2 T_{R1}^2 T_{R2}f^2 + \frac{i}{2}\gamma_1\gamma_2^2 T_{R1}T_{R2}^2 f^4 + \gamma_1\gamma_2^2 s_1 T_{R2}^2 f^4\right)\right], \qquad \text{(A3)}
\end{aligned}
$$

$$
\begin{aligned}
d = \Omega^2\Big[ & R\left(\beta_{22}f^4\gamma_2 k_{12}^2 + \beta_{22}\gamma_1 k_{21}k_{12} + \beta_{21}f^2\gamma_2 k_{12}k_{21} + \frac{1}{f^2}\beta_{21}\gamma_1 k_{21}^2\right) - R^2\left(2\beta_{22}f^3\gamma_1\gamma_2 k_{12} + 2\beta_{21}f\gamma_1\gamma_2 k_{21}\right.\\
& + \frac{4}{f^2}k_{21}^2\gamma_1^2 s_1^2 + 8k_{12}k_{21}\gamma_1\gamma_2 s_1 s_2 f^2 + 4f^6 k_{12}^2\gamma_2^2 s_2^2 + \frac{4i}{f^2}\gamma_1^2 s_1 T_{R1}k_{21}^2 + 4if^2\gamma_1\gamma_2 s_2 T_{R1}k_{21}k_{12} - \frac{1}{f^2}T_{R1}^2\gamma_1^2 k_{21}^2\\
& \left. + 4if^2\gamma_1\gamma_2 s_1 T_{R2}k_{21}k_{12} + 4if^6\gamma_2^2 s_2 T_{R2}k_{12}^2 - 2f^2\gamma_1\gamma_2 T_{R1}T_{R2}k_{21}k_{12} - f^4\gamma_2^2 T_{R2}^2 k_{12}^2\right) + R^3\left(8\gamma_1^2\gamma_2 k_2 1 s_1^2 f\right.\\
& \left. + 8\gamma_1\gamma_2^2 k_{12}s_2^2 f^3 + 8i\gamma_1^2 k_{21}s_1 T_{R1}f + 2\gamma_2\gamma_1^2 k_{21}T_{R1}^2 f\right) + 8i\gamma_1\gamma_2^2 k_{12}T_{R2}s_2 f^3 + 2\gamma_1\gamma_2^3 k_{12}T_{R2}^2 s_2 f^3\Big]\\
& + \Omega^4\Big[\frac{\beta_{22}^2}{4}f^2 k_{12}^2 + \frac{\beta_{21}}{2}\beta_{22}k_{12}k_{21} + \frac{\beta_{21}^2}{4f^2}k_{21}^2 - R\left(\frac{\beta_{22}^2}{2}f\gamma_1 k_{12} - \beta_{21}\beta_{22}f^3\gamma_2 k_{12} - \frac{1}{f}\beta_{21}\beta_{22}\gamma_1 k_{21} - \frac{1}{2}\beta_{21}^2\gamma_2 k_{21}f\right)\\
& + R^2\left(\beta_{21}\beta_{22}\gamma_1\gamma_2 f^2 + \frac{4}{f}\beta_{22}k_{21}\gamma_1^2 s_1^2 + 4\beta_{21}k_{12}f^3\gamma_2^2 s_2^2 + \frac{4}{f}i\beta_{22}k_{21}\gamma_1^2 s_1 T_{R1} - \frac{1}{f}\beta_{22}k_{21}\gamma_1^2 T_{R1}^2\right.\\
& \left. + 4i\beta_{21}f^3 k_{12}\gamma_2^2 s_2 T_{R2} - \beta_{21}f^3 k_{12}\gamma_1^2 T_{R1}^2\right) - R^3\left(4\beta_{22}\gamma_2 s_1^2 f^2 + 4\beta_{21}\gamma_1 s_2^2 f^4 + 4i\beta_{22}\gamma_2 s_1 T_{R1}f^2\right)\\
& - \beta_{22}\gamma_2 T_{R1}^2 f^2 + 4i\beta_{21}\gamma_1\gamma_2^2 s_2 T_{R2}f^2 - \beta_{21}\gamma_1\gamma_2^2 f^4 T_{R2}^2 + R^4\left(16\gamma_1^2\gamma_2^2 s_1^2 s_2^2 f^4 + 16i\gamma_1^2\gamma_2^2 s_1 s_2^2 T_{R1}f^4\right.\\
& - 4\gamma_1^2\gamma_2^2 s_2^2 T_{R1}^2 f^4 + 16i\gamma_1^2\gamma_2^2 s_1^2 s_2 T_{R2}f^4 - 16\gamma_1^2\gamma_2^2 s_1 s_2 T_{R1}T_{R2}f^4 - 4i\gamma_1\gamma_2^2 s_2 T_{R1}T_{R2}f^4\\
& \left. - 4i\gamma_1^2\gamma_2^2 s_1 T_{R1}T_{R2}^2 f^4 + \gamma_1^2\gamma_2^2 T_{R1}^2 T_{R2}^2 f^4\right)\Big] - \Omega^6\Big[\frac{1}{4f}\beta_{21}^2\beta_{22}k_{21} + \frac{1}{4}\beta_{21}^2\beta_{22}^2 k_{12}f - R\left(\frac{1}{4}\beta_{21}\beta_{22}^2\gamma_1\right.\\
& \left. + \frac{1}{4}\beta_{21}^2\beta_{22}\gamma_2 f^2\right) + R^2\left(\beta_{22}^2\gamma_1^2 s_1^2 - \frac{1}{4}\beta_{22}^2\gamma_1^2 T_{R1}^2 + i\beta_{21}^2\gamma_2^2 s_2 T_{R2}f^4 + \frac{1}{4}\beta_{21}^2\gamma_2^2 T_{R2}^2 f^4\right)\Big] + \Omega^8\Big[\frac{1}{16}\beta_{21}^2\beta_{22}^2\Big]. \qquad \text{(A4)}
\end{aligned}
$$


[1] S. M. Jensen, IEEE J. Quan. Electron. **18**, 1580 (1982).
[2] R. Hoffe and J. Chrostowki, Opt. Commun. **57**, 34 (1986).
[3] A. Yariv and P. Yev, *Optical Waves In Crystals* (Wiley, New York, 1984).
[4] A. Yariv, IEEE J. Quan. Electron **9**, 919 (1973).
[5] G. P. Agrawal, *Application of Nonlinear Fibre Optics*, 5th ed. (Academic Press, San Diego, 2012).
[6] N. M. Litchinitser, I. R. Gabitov, and A. I. Maimistov, Phys. Rev. Lett **99**, 113902 (2007).
[7] A. Alu and N. Engheta, *In Negative Refraction Metameterials* (Wiley, New York, 2005).
[8] E. V. Kazantseva, A. I. Maimistov, and S. S. Ozhenko, Phys. Rev. A **80**, 043833 (2009).
[9] T. B. Benjamin and J. E. Feir, J. Fluid Mech. **27**, 417 (1967).
[10] V. I. Bespalov and V. I. Talanov, Pis'ma Zh. Eksp. Teor. Fiz. **3**, 471 (1966).
[11] L. A. Ostrovskii, Sov. Phys. JETP **24**, 797 (1967).
[12] D. Anderson and M. Lisak, Opt. Lett. **9**, 468 (1984).
[13] P. K. Shukla and J. J. Rasmussen, Opt. Lett. **11**, 171 (1986).
[14] K. Nithyanandan, R. Vasantha Jayakantha Raja, and K. Porsezian, J. Opt. Soc. Am. B **30**, 1 (2013).
[15] G. A. Askar'yan, Sov. Phys. JETP **15**, 1088 (1962).
[16] T. Taniuti and H. Washimi, Phys. Rev. Lett. **21**, 209 (1968).
[17] A. Hasewaga, Phys. Rev. Lett. **24**, 1165 (1970).
[18] B. Wu and Q. Niu, Phys. Rev. A **64**, 061603(R) (2001).

[19] V. V. Konotop and M. Salerno, Phys. Rev. A **65**, 021602(R) (2002).
[20] T. Mithun and K. Porsezian, Phys. Rev. A **85**, 013616 (2012).
[21] S. Wen, Y. Wang, W. Su, Y. Xiang, X. Fu, and D. Fan, Phys. Rev. E **73**, 036617 (2006).
[22] Y. Xiang, S. Wen, X.u Dai, and D. Fan, Phys. Rev. E **82**, 056605 (2010).
[23] P. H. Tatsing, A. Mohamadou, C. Bouri, C. G. L. Tiofack, and T. C. Kofane, J. Opt. Soc. Am. B **29**, 3218 (2012).
[24] J. H. Li, K. S. Chiang, and K. W. Chow, J. Opt. Soc. Am. B **28**, 1693 (2011).
[25] R. Ganapathy, K. Senthilnathan, and K. Porsezian, J. Opt. B: Quan. Semiclass. Opt. **6**, s436 (2004).
[26] K. Porsezian, K. Senthilnathan, and S. Devipriya, IEEE J. Quan. Electron. **41**, 789 (2005).
[27] H. zhuo, S. wen, X. dai, Y. hu, Z. tang, Appl. Phys. B **87**, 635 (2007).
[28] W. Shuang-Chun, S. Wen-Hua, Z. Hua, F. Xi-Quan, Q. Lie-Jia, and F. Dian-Yuan, Chin. Phys. Lett. **20**, 852 (2003).
[29] W.-C. Xu, S.-M. Zhang, W.-C. Chen, A.-P. Luo, and S.-H. Liu, Opt. Commun. **199**, 355 (2001).
[30] P. Tchofo Dinda, C. M. Ngabireng, K. porsezian, and B. Kalithasan, Opt. Commun. **266**, 142 (2006).